Case Study

Sediment Propagation in the Porong River below the Sidoardjo Mud Volcano Diversion in Indonesia

Neil Andika[1] and Pierre Y. Julien, M.ASCE[2]

Abstract: The Sidoardjo Mud Volcano in East Java, Indonesia, started on May 29, 2006. The average daily discharge of the mud volcano is 50,000 m^3/day, with a 35% average concentration of sand, silt, and clay. Since 2017, the finer fractions have been diverted to the Madura Strait through the Porong River. The Ginonjo Outlet serves as a point source with a constant discharge of 45 m^3/s and an average sediment concentration of 57,000 mg/L. The settling and transport of fine sediments were studied through field measurements at 106 cross sections over 16 km of the Porong River. At low flow, maximum concentrations decreased from 4,200 to 90 mg/L in the study reach. The two-dimensional mixing and settling model with flocculation resulted in better agreement with the observed data than did models without flocculation. Flocculation tests showed an increase in settling velocity from 0.013 to 0.028 mm/s. Flocculation affected settling of approximately 38% of the total sediment load. The fractions coarser than 92 μm settled within the first 4 km from the point source. **DOI: 10.1061/(ASCE)HY.1943-7900.0001931.**

Author keywords: Mud volcano; Field measurement; Sediment concentration; Flocculation; Two-dimensional mixing and settling.

Introduction

Two geological terms describe piercement structures: mud diapirs and mud volcanoes. A mud diapir is a slow, upward movement of sedimentary mass that does not reach the surface, whereas a mud volcano is a similar geological phenomenon that reaches the surface (Kopf 2002). Several causes of mud volcano formation are a thick sedimentary cover dominated by clay (i.e., smectite, illite, or kaolinite), plastic shale layers and gas accumulation in the subsurface under excessively high pore pressure, rapid subsidence of the sedimentary cover, tectonic activities, and the flow of fluid mass along fractures (Milkov 2000; Blouin et al. 2019). Some reports stated that mud volcano eruptions were triggered by earthquakes with intensities of at least 6 on the Mercalli scale and at a distance less than 100 km from a dormant mud volcano (Mellors et al. 2007; Manga et al. 2009). Dimitrov (2002) stated that the general shape of a mud volcano is a conical mountain form, but other forms such as flat cones, domes, and calderas also have been observed. The size can vary from a few meters up to 500 m in height and the diameter of craters can reach up to 500 m. The worldwide number of mud volcanoes that has been recorded is 900 onshore and 800 offshore (Dimitrov 2002). In Indonesia, mud volcanoes are found in Sumatra, Java, Semau, Rotti, Tanimbar, Sumba, Flores, and Papua (Williams et al. 1984; Breen et al. 1986; Silver et al. 1986; Dimitrov 2002; Kopf 2002).

On May 29, 2006, a mud volcano erupted close to a drilling point of Lapindo Brantas at Sidoardjo, East Java, Indonesia. The mud volcano is called the Sidoardjo Mud Volcano. In 2011, the average eruption rate from the crater of the mud volcano was approximately 50,000 m^3/day (Harnanto 2011). The volumetric sediment concentration of the mud flow gradually decreased from 60% to 30% in the first year (Mazzini et al. 2007). The damage from the Sidoardjo Mud Volcano, which arguably is the largest onshore mud volcano, devastated the surrounding area. The Sidoardjo Mud Volcano caused at least 30,000 refugees (McMichael 2009), buried 10,000 houses, and forced about 23 companies to close (Fig. 1). The total economic losses based on Indonesia Ministry of Public Works' report in 2007 was IDR 7.6 trillion, or about USD 565 million. By March 22, 2007, the impacted area of the Sidoardjo mud flow, as determined by the National Mudflow Disaster Management Team (Tim Nasional Penanggulangan Semburan Lumpur Sidoardjo), had reached 650 ha.

There are two main theories about the origin of the Sidoardjo Mud Volcano. One that it was a natural disaster triggered by the Yogyakarta earthquake on May 27, 2006, is based on geochemical and field results (Mazzini et al. 2007; Sawolo et al. 2009; Lupi et al. 2013). Furthermore, Sawolo et al. (2010) stated that an underground blowout did not occur in an exploration well based on pressure analysis. The second possible cause is an underground blowout due to oil drilling failure of the Banjar Panji-1 exploration well by PT Lapindo Brantas (Manga et al. 2009; Tingay et al. 2008; Mori and Kano 2009; Davies et al. 2007). Some studies claimed that the drilling process induced hydraulic fracturing, and that the Yogyakarta earthquake should be neglected because it did not induce liquefaction of the Kalibeng clay (Davies et al. 2010; Tingay et al. 2015).

The source of the extruded mud was located from the stratigraphy of the Banjar Panji-1 exploration well, which was 150 m from the main crater of Sidoardjo Mud Volcano. The mud had a similar clay mineralogy to a sample from 1,615 to 1,828 m depth, which was in the Upper Kalibeng 1 Formation with a bluish-gray clay, but had more smectite than any samples from a smectite-rich soil in the 1,341–1,432 m interval (Mazzini et al. 2007). Shirzaei et al. (2015) agreed that the mud is from the Upper Kalibeng Formation, but stated that it was supplied by mud from a depth

[1]Postdoctoral, Dept. of Civil and Environmental Engineering, Colorado State Univ., Fort Collins, CO 80523; Faculty Member, Dept. of Civil and Environmental Engineering, Universitas Gadjah Mada, Yogyakarta 55284, Indonesia (corresponding author). ORCID: https://orcid.org/0000-0002-7715-1830. Email: neilah@colostate.edu; neil.andika@ugm.ac.id

[2]Professor, Dept. of Civil and Environmental Engineering, Colorado State Univ., Fort Collins, CO 80523. Email: pierre@engr.colostate.edu

Note. This manuscript was submitted on November 26, 2020; approved on May 30, 2021; published online on August 20, 2021. Discussion period open until January 20, 2022; separate discussions must be submitted for individual papers. This paper is part of the ***Journal of Hydraulic Engineering***, © ASCE, ISSN 0733-9429.

Fig. 1. Mud flow has drowned several settlements and infrastructures in Sidoardjo since 2006. [Image (a) by Neil Andika; images (b–d) courtesy of Candra Kristanto.]

greater than 3.5 km. The main extruded gases from the crater are methane, carbon dioxide, and some hydrocarbons.

Mazzini et al. (2007) stated that in its early stage, the eruption rate of the Sidoardjo Mud Volcano was about 5,000 m^3/day with 60% water content, increased to 180,000 m^3/day in December 10, 2007, and decreased to 110,000 m^3/day after June 2007. Mazzini et al. (2007) also mentioned the presence of an ellipsoidal subsiding area around the mud volcano with an axis of 7×4 km, which had an average subsidence rate of 1–4 cm/day in some areas. It could be caused by the weight of the mud volcano itself or by a void gap left by the extruded mud (Usman et al. 2016).

Typical mud volcanoes last only a few days, but the Sidoardjo Mud Volcano behaves differently. Istadi et al. (2009) predicted that the Sidoardjo Mud Volcano would last 23–35 years, assuming a constant eruption rate of 100,000 m^3/day. Davies et al. (2011) proposed that the lifespan of the mud volcano would be more than 26 years at a flow rate of less than 100,000 m^3/day. Rudolph et al. (2011) predicted, using a Gaussian model, that the Sidoardjo Mud Volcano has a 33% chance of lasting less than 21 years, a 50% chance of lasting less than 40 years, and a 67% chance of lasting less than 84 years.

Because the mud flow cannot be stopped, a containment measure was implemented. However, the mud volume kept increasing, which forced the government to increase the height of embankments and expand the coverage area. The overflow of the mud

Fig. 2. Discharge of the mud mixture into the Porong River at the Ginonjo Outlet. (Image by Neil Andika.)

is diverted to Madura Strait through the Porong River. The river flows about 2 km from the crater of the mud volcano. This action was begun on November 2006 by the Indonesia Ministry of Public Works (Hadimuljono 2008).

Before it is discharged into the Porong River (Fig. 2), the mud is diluted with water to reduce its sediment concentration. This mud

diversion could change the dynamics of the Porong River, increase the sediment concentration in the Porong River, perturb fish and wildlife ecosystems along the Porong River, and cause major sedimentation problems. Several studies have estimated the sediment concentration in the Porong River due to the Sidoardjo Mud Volcano, such as Jennerjahn et al. (2013), Suntoyo et al. (2015), and Bioresita et al. (2018), but the sediment transport and settling by size fractions has not been studied previously. In addition, the possible increase in sedimentation from flocculation of the finer sediment fractions has never been mentioned in previous studies.

The purpose of this research was to better understand the propagation in terms of sediment transport and settling of the Sidoardjo mud from the point source (Ginonjo Outlet) to the Madura Strait. The main objectives of this research were to (1) determine the properties of the mud released into the Porong River, including the relationship between turbidity and suspended sediment concentration and flocculation/settling properties; (2) carry out field measurements of turbidity and sediment concentration along the 16-km reach of the Porong River to the Madura Strait; and (3) develop models for the propagation of suspended sediment with and without flocculation and settling in the Porong River from the steady point source of mud under a range of river flow conditions.

Site Description

The Porong River is a branch of the Brantas River. The Porong River starts at Lengkong Baru Weir in Mojokerto, East Java, and has a total length of about 50 km and an average bed slope of 28 cm/km. At such a flat slope, sedimentation is very likely to occur at low flow. To simplify our analysis, we set our study reach slightly upstream of the Ginonjo Outlet to the estuary into the Madura Strait. The reach length is about 15.8 km (Fig. 3, bold line). The diversion pipes of the Ginonjo Outlet are situated on the left bank of the Porong River.

The Porong station located 2.5 km upstream of the Ginonjo Outlet records the stage and discharge of the Porong River. A flow duration curve at the Porong Station from January 1, 2012 to December 31, 2016, is presented in Fig. 4. The monsoon climate includes a wet season from November to April and a dry season from May to October. The highest hourly discharge between 2012 and 2016 occurred on April 19, 2013 at 14:00 and reached 2,446 m^3/s. The lowest hourly discharge occurred on November 2, 2012 at 22:00, 14.5 m^3/s. Based on the hydrograph of the Porong River,

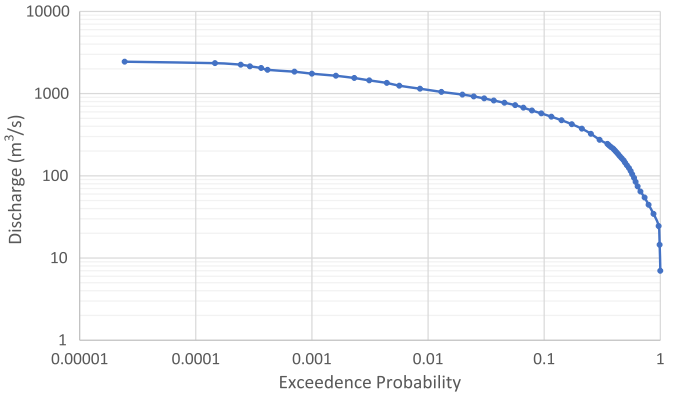

Fig. 4. Flow duration curve of the Porong River.

three flow conditions were considered: low flow $Q_l = 45$ m^3/s, medium flow $Q_m = 250$ m^3/s, and high flow $Q_h = 2{,}500$ m^3/s.

The typical Porong River cross section KP 168 (Fig. 5) is located 30 m downstream of the Ginonjo Outlet. The bankfull width reaches 160 m. Table 1 lists the hydraulic parameters for three flow conditions including discharge (Q), average depth (h), top width (W), flow area (A), energy slope (S_f), average flow velocity (V), and shear velocity (u_*) following methods described by Julien (2018). The low-flow discharge Q_l, which usually occurs during the dry season has flow depth, width, and velocity of 6.3 m, 106 m, and 0.1 m/s, respectively. At such a low velocity, the diverted mud should have more time to settle, and this defines the main condition for this research. The medium flow ($Q_m = 250$ m^3/s), which usually occurs during wet season, has flow depth, width, and average velocity of 6.3 m, 106 m, and 0.57 m/s, respectively. Under this condition, the diverted mud has less time to mix and settle. Under the high flow Q_h, the corresponding flow depth, width, and velocity are 12.2 m, 134 m, 2.16 m/s, respectively. The high average velocity causes the diverted mud to flow quickly to the estuary and have no time to settle in the river. The floods are expected to clean up the sediment deposits from the dry season.

The particle-size distribution of the bed material of the site was investigated. The results are presented in Fig. 6 (Laboratorium Mekanika Tanah dan Batuan 2018). The bed material comprised 0.2% gravel, 43.2% sand, 47.7% silt, and 8.9% clay.

Fig. 3. Plan view of the study reach, indicated by bold line. (Base map courtesy of the Ministry of Public Works and Housing of the Republic of Indonesia.)

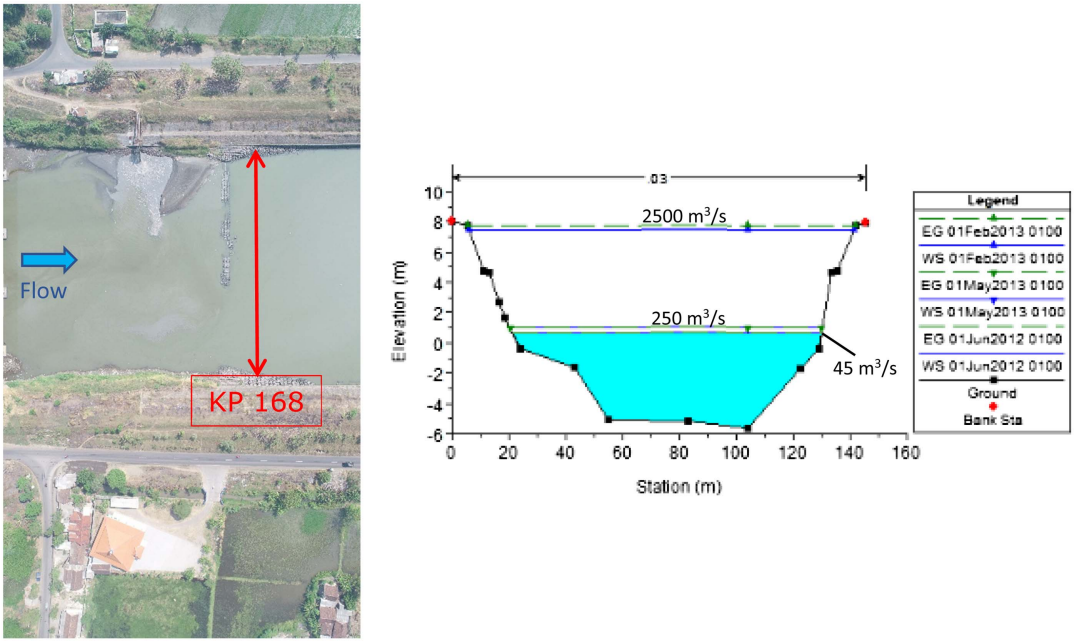

Fig. 5. Cross section of the Porong River. (Image courtesy of Candra Kristanto.)

Table 1. Hydraulic properties of Porong River

Flow condition	Date	Q (m^3)	h (m)	W (m)	A (m^2)	S_f (cm/km)	V (m/s)	u_* (m/s)
Low flow	June 1, 2021	45	3.5	105	370	0.3	0.12	0.01
Medium flow	May 1, 2013	250	3.7	107	400	6.6	0.64	0.05
High flow	February 1, 2013	2500	8.6	135	1160	25	2.15	0.14

Laboratory Experiments

Particle-Size Distribution

The particle-size distribution of samples of the main crater and of the diverted mud at the Ginonjo Outlet are shown in Fig. 6 (Laboratorium Transportasi dan Geoteknik 2018). The extruded mud had 17.1% sand, 44% silt, and 38.9% clay, and the diverted mud of Ginonjo had 0.8% gravel, 13.3% sand, 34.1% silt, and 51.8% clay. The median grain size of the extruded and diverted mud was 8 μ m (medium silt) and 4.7 μm (fine silt), respectively. Thus, the samples consisted mostly of silt and clay particles. The diverted mud at the Ginonjo Outlet had a particle-size distribution comparable to that of the extruded mud at the source, and contained approximately 40% clays. The properties of smectite clays in fluvial environments is not very well known, and was the subject of this study. Physical properties such as turbidity, viscosity/settling, and possible flocculation as the mud becomes diluted in the downstream direction were studied.

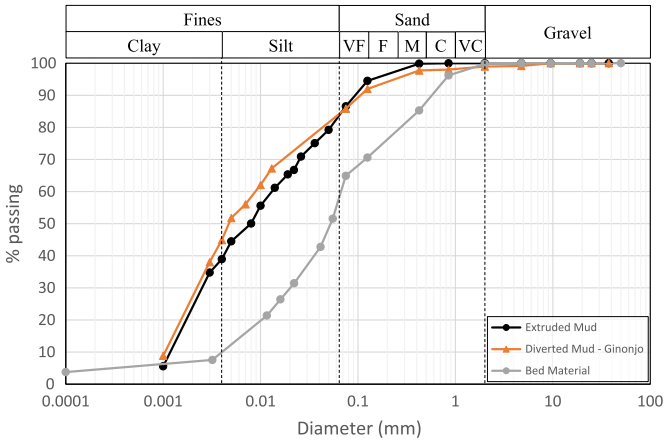

Fig. 6. Particle-size distribution of mud samples and bed materials (VC = very coarse; C = coarse; M = medium; F = fine; and VF = very fine).

Relationship between Turbidity and Sediment Concentration

The relationship between turbidity and sediment concentration was determined from laboratory experiments by diluting a full bottle of sediment sample from the mud reservoir with the Porong River water. The following instruments were used for this laboratory experiment: a Hach 2100P turbidimeter (Hach Company, Jakarta, Indonesia), a Mettler Toledo laboratory scale (Mettle Toledo, Jakarta, Indonesia), a glass beaker, and a 100-mL flask.

The laboratory experiment produced the relationship between turbidity, *Tur*, in nephelometric turbidity units (NTU) and sediment concentration, C, in milligrams/liter as presented in Fig. 7

$$C = 5.3 \times Tur + 24 \quad (1)$$

This relationship is valid for concentrations up to 5,000 mg/L. It was used to convert river turbidity measurements into an estimated sediment concentration in the field measurement programs.

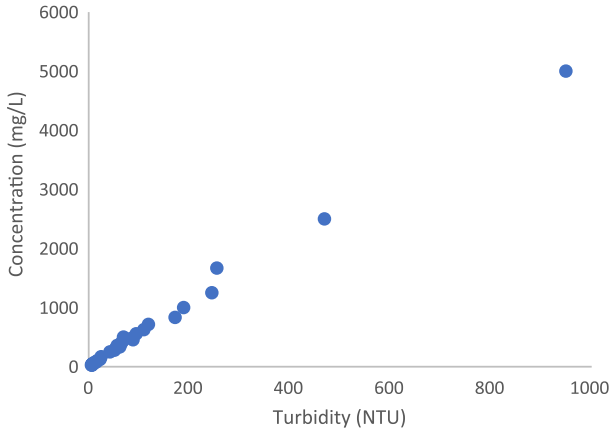

Fig. 7. Relation between turbidity and sediment concentration in the Porong River (the best fit relationship is linear regression $y = 5.3x + 24$).

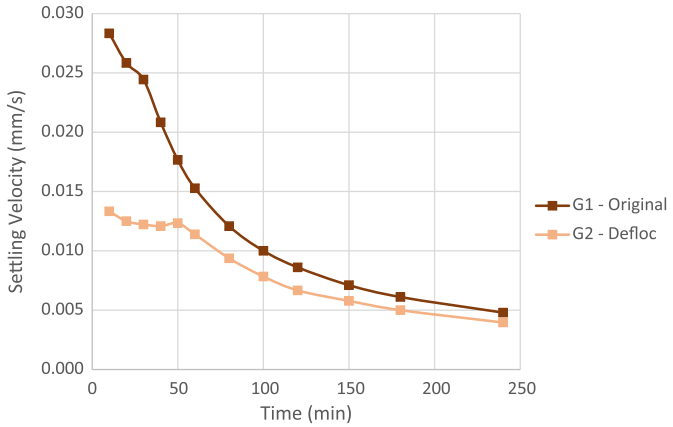

Fig. 8. Results of the flocculation test.

Flocculation Test

Flocculation tests were completed in December 2019 to check the presence of flocculation in the Porong River. Two similar samples were prepared for flocculation tests. A dispersing agent or deflocculant was added to one sample for comparison with the other sample under natural settling conditions. If flocculation occurs in the mixtures, the sample with deflocculant should settle more slowly than the sample without deflocculant. The deflocculant was a mixture of 35.7 g sodium hexametaphosphate and 7.94 g sodium carbonate which was diluted in 1 L distilled water. Then 1 mL of this deflocculant was added per 100 mL of sample (Guy 1969; Vanoni 1962; Julien and Mendelsberg 2003). Two 500 mL samples from the diversion outlet were collected and named G1 (without deflocculant) and G2 (with deflocculant). Both samples were stirred to resuspend all sediment prior to measuring the settling over time. Fig. 8 shows the comparative result of the flocculation test during the first 4 h of the experiment. The settling velocity of the sample mixed with deflocculant, G2, was significantly less than the settling velocity of the original sample, G1. The fastest settling velocity for Samples G1 and G2 were 0.028 and 0.013 mm/s respectively. Therefore, it was considered that the Sidoardjo mud has a tendency to flocculate given that the settling rate differences were much lower than expected. Specifically, settling velocities from 0.005 to 0.03 mm/s at Sidoarjo were 1 order of magnitude lower than the expected 0.15–0.6 mm/s flocculated settling velocity (Julien 2010).

Field Measurements

The field program measured turbidity as a surrogate for sediment concentration (Muller et al. 2014). The sediment concentration was calculated from the measured turbidity using Eq. (1). At the time of the measurements, the discharge of the Porong River was 45 m^3/s, with a flow velocity of 0.16 m/s, shear velocity of 0.01 m/s, and upstream sediment concentration of 56.7 mg/L. The discharge and sediment concentration of the diverted mud at the Ginonjo Outlet were 0.33 m^3/s and 57,000 mg/L, respectively. The river reach was surveyed at 106 cross sections with a distance between cross sections of 150 m. The first cross section of the measurement was located 30 m upstream of Ginonjo Outlet and was intended to capture the undisturbed sediment concentration in the Porong River. The second cross section was 80 m downstream of the Ginonjo Outlet. All following cross sections were spaced 150 m apart (Fig. 9). Four point measurements were taken at each cross section, with a lateral distance between point measurements of 25 m, with a 5-m offset from the left and right bank to avoid additional sediment concentration from the river bank.

Turbidity was measured 1 m below the water surface. An instantaneous horizontal bit–type water sampler was used (WSH-BIT 22, Mona Instrument, Jakarta, Indonesia) with a capacity of 2.2 L (Fig. 10). The turbidity of the sample was measured using a turbidimeter, and the coordinate of the collection point were recorded. Fig. 11 presents pictures of the measurements being conducted in the field.

The turbidity measurements were converted to sediment concentration using Eq. (1). The sediment concentration profiles along the 16-km Porong River are shown in Fig. 12. The measured concentrations for Lines A, B, C, and D had similar patterns, with a very high sediment concentration in the first 2 km, gradually decreasing to about 90 mg/L beyond 3 km from the point source at the Ginonjo Outlet. The highest measured sediment concentration was located in Line C, 4,200 mg/L, followed by Line D (2,704 mg/L), Line B (2,021 mg/L), and Line A (691 mg/L). Lateral mixing near the point source was influenced by a rock sill placed immediately downstream of the Ginonjo Outlet. There also were slight fluctuations beyond 12 km downstream of the Ginonjo Outlet which could be caused by the presence of fish farms in the area.

Advection-Dispersion Equation

Three mixing stages are recognized when sediments or contaminants are discharged from a point source into a river (Fischer et al. 1979; Jung et al. 2009). The first stage is a mixing process controlled by momentum and buoyancy. The second stage is dominated by lateral mixing due to the river turbulence. Longitudinal dispersion spreads the contaminants in the third stage.

The mixing processes in the second stage was analyzed with the advection-diffusion equation. The complete three-dimensional advection-diffusion equation is

$$\frac{\partial C}{\partial t} + u\frac{\partial C}{\partial x} + v\frac{\partial C}{\partial y} + w\frac{\partial C}{\partial z} = \dot{C} + (D + \varepsilon_x)\frac{\partial^2 C}{\partial x^2} + (D + \varepsilon_y)\frac{\partial^2 C}{\partial y^2} + (D + \varepsilon_z)\frac{\partial^2 C}{\partial z^2} \quad (2)$$

where C = mass concentration; D = molecular diffusion; ε = turbulent mixing coefficient; $\dot{C}$ = phase change, and is applied to

Fig. 9. Illustration of the field measurements in the study reach. (Base map © Google Earth.)

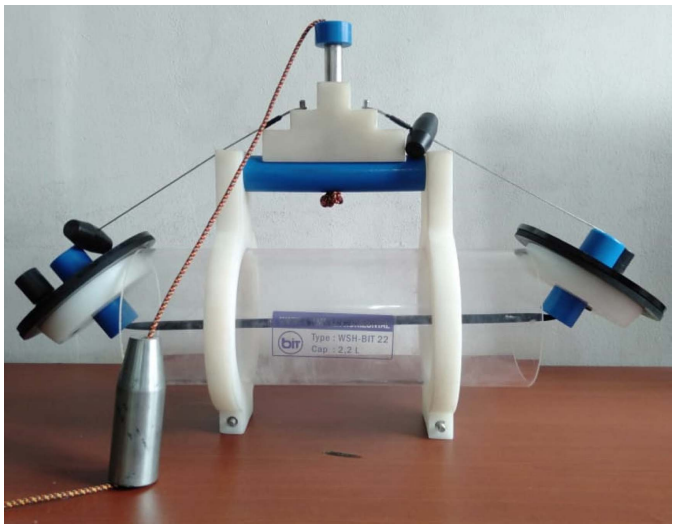

Fig. 10. Water sampler horizontal for field measurements.

nonconservative substances which could undergo an internal mass change such as settling and flocculation. The molecular diffusion D is negligible compared with turbulent mixing in rivers (Julien 2010). The x-, y-, and z-coordinates correspond to the longitudinal, transverse, and vertical directions, respectively ($\varepsilon_x = K_d$, $\varepsilon_y = \varepsilon_t$, and $\varepsilon_z = \varepsilon_v$).

Fischer et al. (1979) proposed empirical functions for the longitudinal dispersion coefficient and vertical and transverse mixing coefficients, K_d, ε_v, and ε_t, respectively, for natural channels, in square meters per second

$$K_d \cong 0.011\frac{U^2W^2}{hu_*} \qquad \varepsilon_v \cong 0.067hu_* \qquad \varepsilon_t \cong 0.6hu_* \tag{3}$$

where U = mean flow velocity; W = channel width; h = flow depth; and $u_* = \sqrt{ghS}$ = shear velocity, where g = gravitational acceleration, and S = energy slope. The dispersion coefficient is more appropriate than the turbulent mixing coefficient in the downstream direction because of the combination of shear flow and velocity gradient, which increases mixing in the downstream direction (Aris 1956). Palu and Julien (2020) investigated the dispersion coefficient.

The first-order approximations of length and time scales, respectively, for longitudinal dispersion and vertical and transverse mixing are

$$X_d = \frac{(500hu_*)}{U} \qquad X_v = \frac{hU}{0.1u_*} \qquad X_t = t_tV = \frac{W^2U}{hu_*} \tag{4}$$

$$t_d \cong \frac{X_d^2}{500hu_*} \qquad t_v \cong \frac{h}{0.1u_*} \qquad t_t = \frac{W^2}{hu_*} \tag{5}$$

The three-dimensional advection-dispersion equation can be simplified in the case of straight channels with the assumption that the most dominant process occurs in the longitudinal x-direction, which for steady point sources implies that $v = w \cong 0$ and $K_d \cong 0$. Furthermore, turbulent flow in natural channels allows us to neglect the molecular diffusion, and after vertical mixing is complete, we can assume that $\varepsilon_v \cong 0$.

Analytical Solution of Nonconservative Advection-Dispersion Equation

For a nonconservative substance, the term $\dot{C}$ in the advection-diffusion equation is not zero, due to internal mass change due to settling and flocculation. For example, the simple one-dimensional solution to the advection-diffusion is

$$\frac{\partial C}{\partial t} = -kC \tag{6}$$

$$C_i = C_0e^{-kt} \tag{7}$$

$$C_i = C_{0i}e^{-\frac{X\omega_i}{hU}} \tag{8}$$

where k = decay rate due to sediment settling; C_{0i} = initial or upstream sediment concentration of fraction i; C_i = downstream

Fig. 11. Photos of the field measurements. (Images courtesy of Candra Kristanto.)

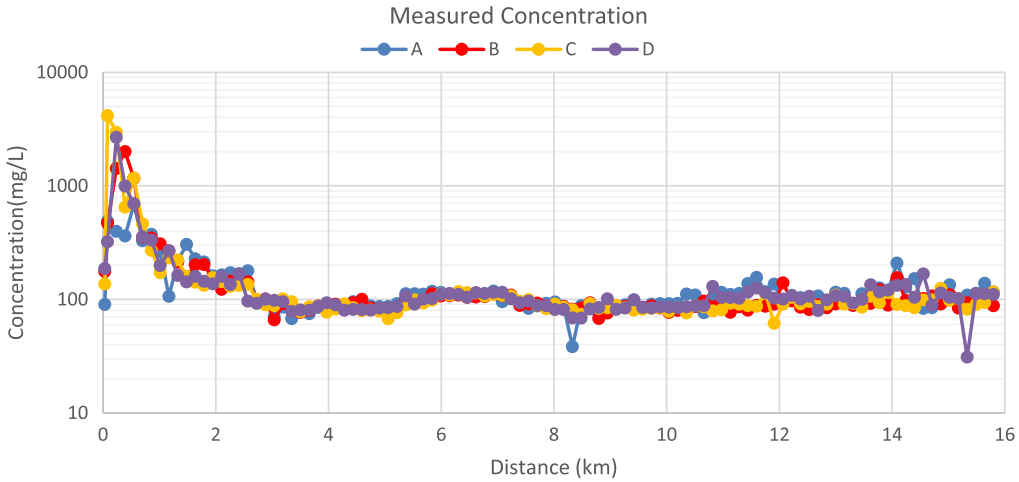

Fig. 12. Measured sediment concentration in the study reach (distance = 0 km is 30 m upstream of the outlet).

sediment concentration of fraction i; X = distance; h = flow depth; U = flow velocity; and ω_i = settling velocity of fraction i. The time t can be defined as X/U. The value of settling rate k for suspended sediment can be defined as $k = \omega/h$, where ω is the settling velocity and h is the flow depth (Julien 2010; Palu and Julien 2019).

The settling velocity for sediment particles as a function of dimensionless particle diameter d_* is

$$\frac{\omega}{\sqrt{(G-1)gd_s}} \cong \frac{8}{d_*^{1.5}}\left(\left(1+\frac{d_*^3}{72}\right)^{1/2}-1\right) \tag{9}$$

$$d_* = d_s\left[\frac{(G-1)g}{\upsilon_m^2}\right]^{1/3} \tag{10}$$

where d_s= particle size; G = specific gravity of particle; and υ_m = kinematic viscosity of fluid (Julien 2010).

If flocculation occurs in a mixture, the settling velocity of the flocculated particles ω_f and the d_{floc} size can be defined as follows:

$$\omega_f = \frac{250}{d_s^2}\omega \tag{11}$$

$$\omega_f = 10(d_{\text{floc}})^{1.5} \tag{12}$$

where d_s = particle size (μm); and ω = settling velocity of disperse particles (mm/s) (Julien 2010).

Analytical Solution of Two-Dimensional Advection-Dispersion Equation

For a conservative substance (assuming no settling of the fine volcano mud), the phase change $\dot{C}$ is assumed to be 0, and the advection-diffusion equation can be simplified into

$$\frac{\partial C}{\partial t} + U\frac{\partial C}{\partial x} = \varepsilon_t\frac{\partial^2 C}{\partial y^2} \tag{13}$$

The analytical solution of the simplified advection diffusion equation for an infinitely wide channel due to continuous mass flux injection $\dot{m}$ is (Julien 2010)

$$C(x,y) = \left[\frac{\dot{m}}{h\sqrt{4\pi\varepsilon_t x U}}\right] e^{-(y^2 U/4\varepsilon_t x)} \tag{14}$$

Narrow rivers are analyzed with the method of superposition. If the sediment source is located at $X = 0$ and both banks are located at $X = \pm L$, by adding imaginary sources at $X = \pm 2L, \pm 4L, \pm 6L, \ldots, \pm nL$, a zero concentration gradient at the boundaries can be achieved (or $\partial C/\partial y = 0$ at $y = 0$ and $y = W$). Assume that y_0 is the location of mass injection or the point source. The solution of the simplified advection diffusion equation after considering the boundaries of the channels is proposed in Eqs. (5.8) and (5.9) of Fischer et al. (1979)

$$\frac{C}{C_b} = \frac{1}{\sqrt{4\pi x'}} \sum_{n=-\infty}^{\infty} \left\{ \exp\left[-\frac{(y' - 2n - y_0')^2}{4x'}\right] + \exp\left[-\frac{(y' - 2n + y_0')^2}{4x'}\right] \right\} \tag{15}$$

$$C_b = \frac{\dot{m}}{UhW}; \qquad \dot{m} = C \times Q; \qquad x' = \frac{x\varepsilon_t}{UW^2}; \qquad y' = \frac{y}{W}; \qquad y_0' = \frac{y_0}{W} \tag{16}$$

where $\dot{m}$ = mass flux injection of sediment, and C_b = fully mixed sediment concentration, which is calculated as

$$C_b = \frac{C_{\text{outlet}} \times Q_{\text{outlet}} + C_{\text{river}} \times Q_{\text{river}}}{Q_{\text{outlet}} + Q_{\text{river}}} \tag{17}$$

Modeling of Suspended Sediment Transport

Two-Dimensional Mixing Model without Settling

The two-dimensional analytical model without settling is helpful to determine how far downstream of the point source the lateral mixing is completed. The model is based on Eqs. (15) and (16) to determine the sediment concentration as a function of the downstream distance x and the lateral distance y. With the diversion outlet located at the left bank, the value of y_0' is 0. The values of $y' = y/W$ for the left bank, centerline, and right bank are 0, 0.5, and 1, respectively. The imaginary sources are located at $n = \pm 4$, ± 3, ± 2, ± 1, and 0. The hydraulic properties of the Porong River (Table 2) were used to estimate the mixing model parameters. The upstream base sediment concentration was unchanged because the focus was to determine the downstream distance for complete lateral mixing.

The simulations were conducted for low-, medium-, and high-flow discharges (Fig. 13). We found that the length scale for complete transverse mixing was 4, 19, and 29 km, respectively, as the discharge increased. Therefore, we concluded that the lateral mixing was complete for the study reach except the upper portion of the reach, particularly at low flow condition. This was corroborated by the field measurements in Fig. 12 which found lateral differences only in the first couple of kilometers immediately downstream of the point source.

At the downstream end of the Porong River under high-flow conditions, the calculated sediment concentrations for the left bank, centerline, and right bank were 70, 64, and 58 mg/L, respectively. This means that the sediment concentration difference between the left bank and right bank was only ±17%.

According to the mixing model under low-flow condition, the concentration should reach equilibrium 4 km downstream of the point source with an average concentration of 470 mg/L. However, the average sediment concentration from the field observations beyond 4 km downstream of the Ginonjo Outlet was only 90 mg/L. There was a 380 mg/L discrepancy in the sediment concentration due to sedimentation in the first 4 km of the study reach. Therefore, sediment settling was incorporated into this two-dimensional model.

Mixing and Settling Model with and without Flocculation

Sediment settling with and without flocculation was incorporated into the mixing model to separate these effects in our analysis. The settling factor was from the solution of advection-diffusion for nonconservative substances

$$e^{-k_i t_{j+1}} = \frac{C_{i,j+1}}{C_{i,j}} \tag{18}$$

where $C_{i,j+1}$ = sediment concentration of fraction i at location $j + 1$; $C_{i,j}$ = sediment concentration of fraction i at location j; $k_i = \omega_i/h$ = settling rate of fraction i, where ω_i = settling velocity of fraction i, and h = flow depth; and $t = X/U$ = time, where X = river length and U = flow velocity.

After the sediment concentration at point j, C_j, from Eq. (18) is substituted into Eq. (15), and the numerical model for advection-dispersion in a river with settling becomes

$$C_{i,j+1} = C_{b,i} e^{-k_i t_{j+1}} \left(\frac{1}{\sqrt{4\pi x_j'}} \sum_{n=-\infty}^{\infty} \left\{ \exp\left[-\frac{(y' - 2n - y_0')^2}{4x_j'}\right] + \exp\left[-\frac{(y' - 2n + y_0')^2}{4x_j'}\right] \right\} \right) \tag{19}$$

The sediment concentration propagation was computed by size fractions from the particle-size distribution to better understand the settled and unsettled portion of the diverted mud. The total suspended sediment concentration is

$$C = \sum \Delta p_i C_i \tag{20}$$

where Δp_i = relative weight of fraction i; and C_i = suspended sediment concentration for fraction i.

Table 2. Coefficients, length and time scales of longitudinal dispersion, and vertical and transverse mixing of Porong River

Flow condition	K_d (m²/s)	ε_v (m²/s)	ε_t (m²/s)	X_d (m)	X_v (m)	X_t (m)	t_d (s)	t_v (s)	t_t (s)
Low flow	85	0.02	0.20	1,420	43	3,920	11,800	355	32,660
Medium flow	95	0.03	0.23	300	240	19,260	460	370	30,100
High flow	330	0.09	0.80	290	1,200	29,250	145	560	13,600

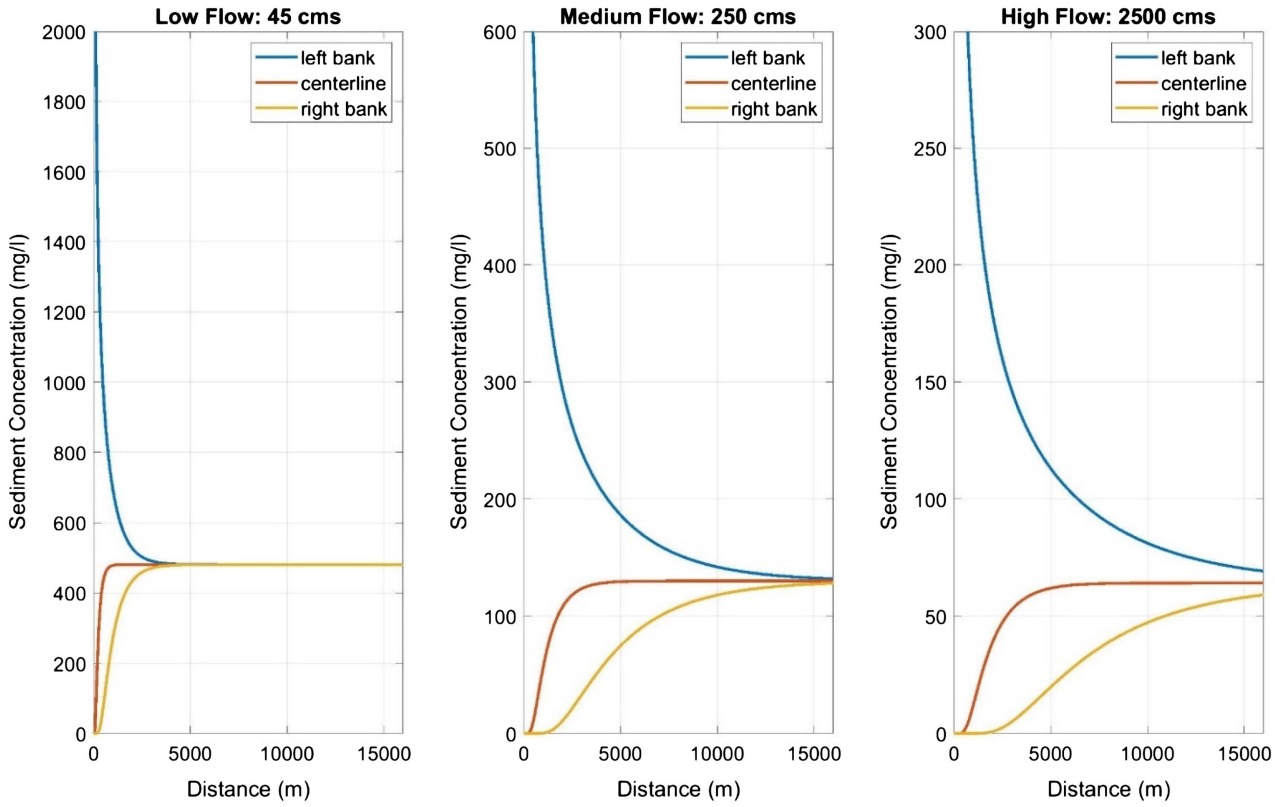

Fig. 13. Sediment propagation at left bank, centerline, and right bank in Porong River for three flow conditions.

Table 3 summarizes the sediment propagation along the Porong River. Column 1 lists the name of the fraction i, Column 2 lists the particle size of fraction i, and Column 3 lists the relative weight of fraction i, Δp_i. Columns 1, 2, and 3 were derived from the particle-size distribution of the diverted mud in Fig. 6. Column 4 lists the settling velocity of fraction i, which was calculated using Eqs. (9) and (10). Column 5 lists the settling rate of fraction i, $k_i = \omega_i/h_i$. The sediment concentration of fraction i and the total concentration were calculated using Eqs. (19) and (20). The parameters of the advection diffusion equation, C_b, y', y'_0, and x', are from Eq. (16).

A floc class, Class 14, was added to introduce the flocculated particles into the mathematical model. The floc class had a flocculated settling velocity of 0.28 mm/s and a floc size of 92 μ m. The properties of this floc class were different from those determined by the laboratory experiment. The flocculated settling velocity from the laboratory experiment underestimated the flocculated settling rate in the field. This was because visual information in the laboratory experiment was controlled by the finest size fractions of the particle-size distribution. The best agreement with the field measurements was obtained using Eqs. (11) and (12) to determine the flocculated settling velocity. Laboratory tests remain important to determine whether or not flocculation occurs. Calculations by size fractions and comparisons with field measurements therefore are recommended.

The relative weight of fraction i, Δp_i, was based on the percentage of retained particle per class with some modification through trial and error. The particle distribution was modified mainly for classes finer than 13 μm by reducing the weight of the fraction and adding it into a floc class. The upper limit of the modified class was 13 μm (Class 7) because the flocculation usually occurs with the particles smaller than 40 μm. The modification of the weight of the class will vary thoughout time because a number of variables affect the flocculation of smectite clay, such as salinity, flow velocity, turbulence, clay properties, and sediment mixtures distribution. However, in this study, the average reduction of the weight of the class that produced the best agreement with the field measurements was 50%, which applied for Class 7 to Class 13.

The class with the highest weight was the floc class of 92 μm, with approximately 38%, followed by fractions of 75 μm, with 12%. Flocculation thus increased the rate of settling such that approximately 50% of the sediment settled at a rate comparable to that of fine sands, and the effective clay fraction was reduced to about 22% of the sediment mixture.

The results of the mixing and settling model were compared with the field measurements (Fig. 14). At the end of the study reach, the sediment concentration of the model without flocculation was 195 mg/L, which was about 2 times higher than the field observations. However, including flocculation in the model decreased the downstream concentration to 90 mg/L, which closely matched the field observations of 80–100 mg/L. The fractions coarser than sand settled within the first 300 m of the Porong River. The silt fractions of 13 μm and 10 μm mostly settled within the first 10 km, leaving only small amounts of the nonflocculated finer fractions of 7, 5, and 4 μm still in suspension until the end of the study reach. The fractions of 3 and 1 μm were the only significant fractions in suspension near the end of the Porong River, with concentrations of 24 and 54 mg/L, respectively.

The percentage of the sedimentation in the Porong River was calculated using the trap efficiency equation

$$T_E = \frac{C_j - C_{j+1}}{C_j} \tag{21}$$

The overall percentage of settled sediment in the Porong River under low flow conditions was about 98%. The agreement between the observed data and the two-dimensional mixing and settling

Table 3. Classes of diverted mud with parameters and sediment concentrations at certain distances from Ginonjo Outlet

					C (mg/L)							
Class	d_s (mm)	dP_i (%)	ω (m/s)	K (L/s)	$X = 0$ m	$X = 100$ m	$X = 300$ m	$X = 500$ m	$X = 1{,}000$ m	$X = 3{,}000$ m	$X = 5{,}000$ m	$X = 10{,}000$ m	$X = 15{,}000$ m	$X = 15{,}800$ m
1	4.75	0.9	0.26	0.075	39	0	0	0	0	0	0	0	0	0
2	2	0.6	0.17	0.048	23	0	0	0	0	0	0	0	0	0
3	0.85	0.6	0.10	0.030	25	0	0	0	0	0	0	0	0	0
4	0.425	3.0	0.06	0.019	123	0	0	0	0	0	0	0	0	0
5	0.125	6.0	0.02	0.004	243	6	0	0	0	0	0	0	0	0
6	0.075	12.4	0.01	0.002	505	117	2	0	0	0	0	0	0	0
7	0.013	8.3	1.9×10^{-04}	5.5×10^{-05}	339	324	107	71	38	10	4	0	0	0
8	0.01	2.2	1.1×10^{-04}	3.2×10^{-05}	91	89	30	21	12	5	3	1	0	0
9	0.007	2.6	5.5×10^{-05}	1.6×10^{-05}	105	104	36	26	16	9	6	3	2	2
10	0.005	2.8	2.8×10^{-05}	8.1×10^{-06}	114	113	40	29	19	11	10	7	5	5
11	0.004	2.7	1.8×10^{-05}	5.2×10^{-06}	112	112	40	29	19	12	11	9	7	7
12	0.003	7.2	1.0×10^{-05}	2.9×10^{-06}	294	293	105	76	51	33	31	27	24	24
13	0.001	11.7	1.1×10^{-06}	3.2×10^{-07}	478	478	172	125	84	57	56	55	54	54
14	0.092	38.9	2.8×10^{-04}	8.1×10^{-05}	1,588	183	1	0	0	0	0	0	0	0
Total	—	100	—	—	4,079	1,819	535	376	240	138	120	102	92	91

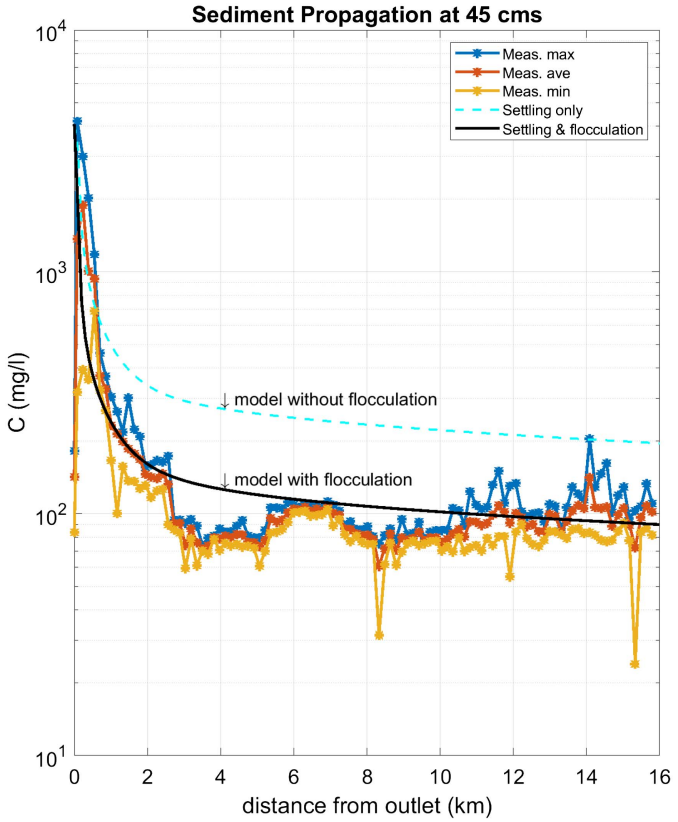

Fig. 14. Measurement data and results of model with flocculation and without flocculation.

model with flocculation means that the model can be used to predict the sediment propagation in the Porong River due to diversion from the Sidoarjo Mud Volcano. More details of this analysis were given by Andika (2021).

Conclusion

This paper investigated the propagation of diluted muds in rivers. The suspended sediment propagation in the Porong River after the diversion of the Sidoardjo Mud Volcano was modeled using the advection-diffusion equation for comparison with field observations. The mud properties were determined by laboratory experiments. The diverted mud was dominated by silt and smectite clay particles with a median grain size of 4.7 μm. A relationship between turbidity and sediment concentration in the Porong River was established as $C = 5.3 \times Tur + 24$. It was concluded that turbidity measurements can be used as a surrogate for sediment concentration measurements. It also was found in the laboratory experiments that the mud tends to flocculate with a settling velocity of 0.028 mm/s, which is representative of the smaller fractions of the mixture. Thus, flocculation tests in the laboratory can detect whether flocculation will occur. However, the laboratory experiments for flocculated settling velocity of smectite clay usually underestimated the flocculated settling velocity in the field because the laboratory experiments were controlled by the finest fraction.

The sediment propagation and settling of the mud diversion from the Sidoardjo Mud Volcano in the Porong River can be predicted accurately by calculating the advection and diffusion of sediment by size fractions with modification, and must include the settling and flocculation factors. The calculation by size fraction

is necessary to analyze the flocculation processes for the fine fractions. In addition, the modification of the particle distribution will vary, and depends on the flocculation properties of the clay, the sediment distribution, and the river properties.

The modeled distribution of sediment concentration along 16 km of the Porong River matched the field observations. The sediment fractions coarser than medium silt, including the flocculated particles, settled within the first 4 km of the study reach. Only the nonflocculated clay fractions finer than 3 μm remained in suspension at the downstream end of the study reach of the Porong River. Thus, the two-dimensional advection-diffusion model coupled with sediment settling can be used to model the sediment concentration distribution in a river due to a point source of mud or fine particles.

Data Availability Statement

Some or all data, models, or code that support the findings of this study are available from the corresponding author upon reasonable request, including the hydraulic properties and hydrology of the Porong River, the laboratory experiment data, and the observed turbidity.

Acknowledgments

The authors gratefully acknowledge that this work has been made possible with the support of the Indonesian Endowment Fund for Education (LPDP) and Pusat Pengendalian Lumpur Sidoardjo (PPLS) (the Sidoardjo Mud Control Center) of the Ministry of Public Works and Housing of the Republic of Indonesia.

References

Andika, N. 2021. "Propagation of the Sidoardjo Mud in the Porong River, East Java, Indonesia." Ph.D. dissertation, Dept. of Civil and Environmental Engineering, Colorado State Univ.

Aris, R. 1956. "On the dispersion of a solute in a fluid flowing through a tube." *Proc. R. Soc. London, Ser. A Math. Phys. Sci.* 235 (1200): 67–77. https://doi.org/10.1098/rspa.1956.0065.

Bioresita, F., C. B. Pribadi, H. S. Firdaus, T. Hariyanto, and A. Puissant. 2018. "The use of Sentinel-2 imagery for total suspended solids (TSS) estimation in Porong River, Sidoardjo." *Elipsoida: Jurnal Geodesi dan Geomatika* 1 (1): 1–6.

Blouin, A., P. Imbert, N. Sultan, and J.-P. Callot. 2019. "Evolution model for the Absheron Mud Volcano: From in-situ observation to numerical modeling." *J. Geophys. Res. Earth Surf.* 124 (3): 766–794. https://doi.org/10.1029/2018JF004872.

Breen, N. A., E. A. Silver, and D. M. Hussong. 1986. "Structural styles of an accretionary wedge south of the Island of Sumba, Indonesia, revealed by SeaMARC II side scan sonar." *Geol. Soc. Am. Bull.* 97 (10): 1250–1261. https://doi.org/10.1130/0016-7606(1986)97<1250:SSOAAW>2.0.CO;2.

Davies, R., M. Manga, M. Tingay, S. Lusianga, and R. Swarbrick. 2010. "Discussion: Sawolo et al. (2009) the Lusi mud volcano controversy: Was it caused by drilling?" *Mar. Pet. Geol.* 27 (7): 1651–1657. https://doi.org/10.1016/j.marpetgeo.2010.01.019.

Davies, R. J., S. A. Mathias, R. E. Swarbrick, and M. J. Tingay. 2011. "Probabilistic longevity estimate for the LUSI mud volcano, East Java." *J. Geol. Soc.* 168 (2): 517–523. https://doi.org/10.1144/0016-76492010-129.

Davies, R. J., R. E. Swarbrick, R. J. Evans, and M. Huuse. 2007. "Birth of a mud volcano: East Java, 29 May 2006." *GSA Today* 17 (2): 4–9. https://doi.org/10.1130/GSAT01702A.1.

Dimitrov, L. I. 2002. "Mud volcanoes—The most important pathway for degassing deeply buried sediments." *Earth Sci. Rev.* 59 (1–4): 49–76. https://doi.org/10.1016/S0012-8252(02)00069-7.

Fischer, H. B., E. J. List, R. C. Y. Koh, J. Imberger, and N. H. Brooks. 1979. *Mixing in inland and coastal waters*. New York: Academic Press.

Guy, H. P. 1969. "Laboratory theory and methods for sediment analysis." In *United States Geological Survey techniques of water resources investigations, Book 5*. Washington, DC: United States Government Printing Office.

Hadimuljono, M. B. 2008. *Sidoardjo's hot mudflow catastrophe: Lesson from a disaster*. Jakarta, Indonesia: Spirit Komunika Group.

Harnanto, A. 2011. *Peranan Kali Porong dalam mengalirkan lumpur Sidoardjo ke laut*. Surabaya, Indonesia: Badan Pelaksana - Badan Penanggulangan Lumpur Sidoardjo (BAPEL-BPLS).

Istadi, B. P., G. H. Pramono, P. Sumintadireja, and S. Alam. 2009. "Modeling study of growth and potential geohazard for LUSI mud volcano: East Java, Indonesia." *Mar. Pet. Geol.* 26 (9): 1724–1739. https://doi.org/10.1016/j.marpetgeo.2009.03.006.

Jennerjahn, T. C., T. Jänen, C. Propp, S. Adi, and S. P. Nugroho. 2013. "Environmental impact of mud volcano inputs on the anthropogenically altered Porong River and Madura Strait coastal waters, Java, Indonesia." *Estuarine Coastal Shelf Sci.* 130 (Sep): 152–160. https://doi.org/10.1016/j.ecss.2013.04.007.

Julien, P. Y. 2010. *Erosion and sedimentation*. 2nd ed. New York: Cambridge University Press.

Julien, P. Y. 2018. *River mechanics*. 2nd ed. New York: Cambridge University Press.

Julien, P. Y., and A. Mendelsberg. 2003. *Sediment in Arroyo Pasajero and San Luis Canal*. Fort Collins, CO: Colorado State Univ.

Jung, S. H., I. W. Seo, Y. D. Kim, and I. Park. 2009. "Feasibility of velocity-based method for transverse mixing coefficients in river mixing analysis." *J. Hydraul. Eng.* 145 (11): 04019040. https://doi.org/10.1061/(ASCE)HY.1943-7900.0001638.

Kopf, A. J. 2002. "Significance of mud volcanism." *Rev. Grophys.* 40 (2): 1005. https://doi.org/10.1029/2000RG000093.

Laboratorium Mekanika Tanah dan Batuan. 2018. *Laporan hasil uji analisa pembagian butir*. Surabaya, Indonesia: Institut Teknologi Sepuluh November—Fakultas Teknik Sipil dan Lingkungan.

Laboratorium Transportasi dan Geoteknik. 2018. *Laporan hasil tes laboratorium PPLS (Pusat Pengendalian Lumpur Sidoardjo)*. Surabaya, Indonesia: Institut Teknologi Sepuluh November–Fakultas Vokasi.

Lupi, M., E. H. Saenger, F. Fuchs, and S. A. Miller. 2013. "Lusi mud eruption triggered by geometric focusing of seismic waves." *Nat. Geosci.* 6 (8): 642–646. https://doi.org/10.1038/ngeo1884.

Manga, M., M. Brumm, and M. L. Rudolph. 2009. "Earthquake triggering of mud volcanoes." *Mar. Pet. Geol.* 26 (9): 1785–1798. https://doi.org/10.1016/j.marpetgeo.2009.01.019.

Mazzini, A., H. Svensen, G. G. Akhmanov, G. Aloisi, S. Planke, A. Malthe-Sørenssen, and B. Istiadi. 2007. "Triggering and dynamic evolution of the LUSI mud volcano, Indonesia." *Earth Planet. Sci. Lett.* 261 (3–4): 375–388. https://doi.org/10.1016/j.epsl.2007.07.001.

McMichael, H. 2009. "The Lapindo mudflow disaster: Environmental, infrastructure and economic impact." *Bull. Indonesian Econ. Stud.* 45 (1): 73–83. https://doi.org/10.1080/00074910902836189.

Mellors, R., D. Kilb, A. Aliyev, A. Gasanov, and G. Yetirmishli. 2007. "Correlations between earthquakes and large mud volcano eruptions." *J. Geophys. Res.* 112 (B4): B04304. https://doi.org/10.1029/2006JB004489.

Milkov, A. V. 2000. "Worldwide distribution of submarine mud volcanoes and associated gas hydrates." *Mar. Geol.* 167 (1–2): 29–42. https://doi.org/10.1016/S0025-3227(00)00022-0.

Mori, J., and Y. Kano. 2009. "Is the 2006 Yogyakarta earthquake related to the triggering of the Sidoarjo, Indonesia mud volcano?" *J. Geogr.* 118 (3): 492–498. https://doi.org/10.5026/jgeography.118.492.

Muller, M., G. De Cesare, and A. J. Schleiss. 2014. "Continuous long-term observation of suspended sediment transport between two pumped-storage reservoirs." *ASCE J. Hydraul. Eng.* 140 (5): 05014003. https://doi.org/10.1061/(ASCE)HY.1943-7900.0000866.

Palu, M., and P. Y. Julien. 2019. "Case study: Modeling the sediment load of the Doce River after the Fundão Tailings Dam collapse, Brazil." *J. Hydraul. Eng.* 145 (5): 05019002. https://doi.org/10.1061/(ASCE)HY.1943-7900.0001582.

Palu, M., and P. Y. Julien. 2020. "Test and improvement of 1D routing algorithms for dam-break floods." *J. Hydraul. Eng.* 146 (6): 04020043. https://doi.org/10.1061/(ASCE)HY.1943-7900.0001755.

Rudolph, M. L., L. Karlstrom, and M. Manga. 2011. "A prediction of the longevity of the Lusi mud eruption, Indonesia." *Earth Planet. Sci. Lett.* 308 (1–2): 124–130. https://doi.org/10.1016/j.epsl.2011.05.037.

Sawolo, N., E. Sutriono, B. P. Istiadi, and A. B. Darmoyo. 2009. "The LUSI mud volcano triggering controversy: Was it caused by drilling?" *Mar. Pet. Geol.* 26 (9): 1766–1784. https://doi.org/10.1016/j.marpetgeo.2009.04.002.

Sawolo, N., E. Sutriono, B. P. Istiadi, and A. B. Darmoyo. 2010. "Was Lusi caused by drilling?–Authors reply to discussion." *Mar. Pet. Geol.* 27 (7): 1658–1675. https://doi.org/10.1016/j.marpetgeo.2010.01.018.

Shirzaei, M., M. L. Rudolph, and M. Manga. 2015. "Deep and shallow sources for the Lusi mud eruption revealed by surface deformation." *Geophys. Res. Lett.* 42 (13): 5274–5281. https://doi.org/10.1002/2015GL064576.

Silver, E. A., N. A. Breen, H. Prasetyo, and D. M. Hussong. 1986. "Multibeam study of the Flores backarc thrust belt, Indonesia." *J. Geophys. Res.* 91 (B3): 3489–3500. https://doi.org/10.1029/JB091iB03p03489.

Suntoyo, H. Ikhwani, M. Zikra, N. A. Sukmasari, G. Angraeni, H. Tanaka, M. Umeda, and S. Kure. 2015. "Modelling the COD, TSS, phosphate and nitrate distribution due to the Sidoardjo mud flow into Porong River estuary." *Procedia Earth Planet. Sci.* 14: 144–151. https://doi.org/10.1016/j.proeps.2015.07.095.

Tingay, M., O. Heidbach, R. Davies, and R. Swarbrick. 2008. "Triggering of the Lusi mud eruption: Earthquake versus drilling initiation." *Geology* 36 (8): 639–642. https://doi.org/10.1130/G24697A.1.

Tingay, M. R. P., M. L. Rudolph, M. Manga, R. J. Davies, and C.-Y. Wang. 2015. "Initiation of the Lusi mudflow disaster." *Nat. Geosci.* 8 (7): 493–494. https://doi.org/10.1038/ngeo2472.

Usman, E., M. Salahuddin, D. A. S. Ranawijaya, and J. P. Hutagaol. 2016. "Lokasi pengendapan akhir dan evaluasi pengelolaan Lumpur Porong." Accessed February 19, 2018. www.mgi.esdm.go.id/content/lokasi-pengendapan-akhir-dan-evaluasi-pengelolaan-lumpur-porong.

Vanoni, V. A. 1962. *Sedimentation Engineering*. ASCE Manual and Reports on Engineering Practice No. 54. Reston, VA: ASCE.

Williams, P. R., C. J. Pigram, D. B. Dow, and Amiruddin. 1984. "Melange production and the importance of shale diapirsm in accretionary terrains." *Nature* 309 (5964): 145–146. https://doi.org/10.1038/309145a0.